

# A *PTCH1* Homolog Transcriptionally Activated by p53 Suppresses Hedgehog Signaling\*

Received for publication, July 22, 2014, and in revised form, October 6, 2014. Published, JBC Papers in Press, October 8, 2014, DOI 10.1074/jbc.M114.597203

Jon H. Chung<sup>1</sup>, Andrew R. Larsen, Evan Chen, and Fred Bunz<sup>2</sup>

From the Department of Radiation Oncology and Molecular Radiation Sciences, The Kimmel Cancer Center at Johns Hopkins, Baltimore, Maryland 21231

**Background:** p53 activates transcription of downstream target genes that contribute to tumor suppression.

**Results:** The expression of *PTCH53*, a structural and functional homolog of *PTCH1*, is highly responsive to p53 in diverse cells and tissues.

**Conclusion:** p53 can suppress canonical Hedgehog signaling via induction of *PTCH53*.

**Significance:** *PTCH53* is a new mediator by which p53 can suppress oncogenic Hedgehog signals.

The p53-mediated responses to DNA damage and the Hedgehog (Hh) signaling pathway are each recurrently dysregulated in many types of human cancer. Here we describe *PTCH53*, a p53 target gene that is homologous to the tumor suppressor gene *PTCH1* and can function as a repressor of Hh pathway activation. *PTCH53* (previously designated *PTCHD4*) was highly responsive to p53 *in vitro* and was among a small number of genes that were consistently expressed at reduced levels in diverse *TP53* mutant cell lines and human tumors. Increased expression of *PTCH53* inhibited canonical Hh signaling by the G protein-coupled receptor SMO. *PTCH53* thus delineates a novel, inducible pathway by which p53 can repress tumorigenic Hh signals.

The tumor suppressor p53 can activate numerous target genes in response to DNA damage. The human genome contains at least 500 experimentally identified p53 binding sites (1–3), and ~100 genes have been rigorously demonstrated to be directly transactivated by p53 (4). p53 mediates cell cycle arrest and apoptosis by inducing the expression of prototypical target genes, such as *CDKN1A* (also known as *P21* (5)) and *BAX* (6). More recent studies have expanded the repertoire of p53 target genes and have accordingly implicated p53 in diverse processes, such as senescence, autophagy, oxidative metabolism, angiogenesis, invasion, and stem cell maintenance (7).

The composition of the p53-induced transcriptome varies considerably in different experimental systems. In cultured cells, the relative expression of p53 target genes is highly cell line- and cell type-dependent. These different expression patterns result in distinct cellular phenotypes (4, 8). Notably, many

p53 target genes that were identified and extensively characterized *in vitro* do not appear to be differentially expressed in *TP53* wild type and *TP53* mutant human tumors (8, 9).

In this report, we describe the identification and initial functional characterization of *PTCH53*, a p53 target gene that can inhibit signaling by the canonical Hh<sup>3</sup> pathway. *PTCH53* is a homolog of the tumor suppressor *PTCH1*, the prototypical repressor of Hh signaling by the human G protein-coupled receptor SMO. We demonstrate that *PTCH53* was highly responsive to wild type p53 in large and diverse panels of cultured human cells and expressed at significantly decreased levels in *TP53* mutant human tumors. Like *PTCH1*, *PTCH53* could suppress Hh signals via inhibition of SMO, suggesting a heretofore unrecognized link between these two important tumor suppressor pathways.

## EXPERIMENTAL PROCEDURES

**Cell Lines**—HCT116, RKO, SW48, and DLD-1 colorectal cancer cells and their isogenic derivatives (10) were cultured in McCoy's 5A medium supplemented with 10% fetal bovine serum (FBS) and penicillin/streptomycin. The immortalized human retinal epithelial cell line hTERT-RPE1 was cultured in DMEM/F-12 medium supplemented with 10% FBS and penicillin/streptomycin. Ccd-18Co and IMR-90 (ATCC) human fibroblast cells were cultured in DMEM supplemented with 10% FBS and penicillin/streptomycin. DAOY medulloblastoma cells were cultured in minimum essential medium with 10% FBS and penicillin/streptomycin. C3H10T1/2 mouse fibroblasts (ATCC) and *SMO*<sup>-/-</sup> mouse embryonic fibroblasts (a gift from Dr. James Kim) were grown in DMEM with 10% FBS penicillin/streptomycin.

**Rapid Amplification of cDNA Ends (RACE) and Protein Alignment**—RACE in the 5' orientation was performed with the FirstChoice RLM-RACE kit (Ambion), using the gene-specific outer primer 5'-GAGGCCGAAGGTGATTGTC-3' and the gene-specific inner primer 5'-CCTCCACCAGATCCAGCTC-3'. The full sequence of *PTCH53* with the newly identified

\* This work was supported, in whole or in part, by National Institutes of Health Grants R01CA157535 (to F. B.), P30CA006973 (to the Johns Hopkins gastrointestinal cancer SPORE), and P50CA062924 (to the Sidney Kimmel Comprehensive Cancer Center).

The nucleotide sequence(s) reported in this paper has been submitted to the GenBank™/EBI Data Bank with accession number(s) KJ534581.

<sup>1</sup> Supported in part by the AACR-Fight Colorectal Cancer fellowship.

<sup>2</sup> To whom correspondence should be addressed: Dept. of Radiation Oncology and Molecular Radiation Sciences, The Kimmel Cancer Center at Johns Hopkins, 1550 Orleans St., Baltimore, MD 21231. Tel.: 410-502-7941; Fax: 410-502-2821; E-mail: fredbunz@jhmi.edu.

<sup>3</sup> The abbreviations used are: Hh, Hedgehog; ShhN, processed Sonic Hedgehog ligand; Gli-luc, GLI-activated luciferase reporter; qPCR, quantitative PCR.

ified exons 1 and 2 has been deposited in GenBank™ (accession no. KJ534581). The alignment of the predicted PTCH53 protein and PTCH1 was performed with the Basic Alignment Search Tool (BLASTP, version 2.2.30+), which identified amino acid similarities and identities as well as gaps within regions of homology.

**p53 Activation and Chromatin Immunoprecipitation**—Nutlin-3 (also known as nutlin-3a; Enzo Life Sciences) was dissolved in DMSO to a concentration of 10 mM. Cells were treated with a final concentration of 10  $\mu$ M. For activation of p53 by radiation, cells were exposed to a  $^{137}\text{Cs}$   $\gamma$ -ray source at a dose rate of 100 centigrays/min. For chromatin immunoprecipitation experiments, cells were harvested 24 h after treatment and processed with the EZ-ChIP kit (Millipore) according to the manufacturer's instructions. Anti-p53 antibody (monoclonal DO1) was purchased from Santa Cruz Biotechnology, Inc. Primers used for amplification of the p53 binding site BS1 in *PTCH53* were as follows: forward, 5'-AAAACAAGGAGAGGATGTTCTTTG-3'; reverse, 5'-TTCTCTGCTACTTCTCTGCCATA-3'. The *PTCH53* BS2 site was probed with 5'-CACCGAGATGAAGGGCTAGA-3' (forward) and 5'-ACCTCCATGCGCTCCTACTA-3' (reverse). *CDKN1A* p53 binding site primers were 5'-CACCTTTCACCATTTCCCCTA-3' (forward) and 5'-GCAGCCCAAGGACAAAATAG-3' (reverse).

**Quantitative Real-time PCR**—RNA was extracted and purified with TRIzol (Life Technologies) and treated with DNase I (Thermo Scientific). First strand cDNA synthesis was performed with the Maxima First Strand cDNA synthesis kit (Thermo Scientific). Each sample was analyzed in triplicate by quantitative RT-PCR with oligonucleotide primers using Maxima SYBR Green/Rox Master Mix (Thermo Scientific) and an ABI PRISM 7900HT sequence detection system (Applied Biosystems). Relative gene expression was calculated using the  $2^{-\Delta\Delta C_t}$  method using *GAPDH* for normalization.  $C_t$  values greater than 35 were considered not detectable. The following primer pairs were used: *PTCH53*, 5'-AAGCCAGCTC-TATTCCGACTTAC-3' (forward) and 5'-ACTTGACCCGCTGATCTTTG-3' (reverse); *CDKN1A*, 5'-ACAGCAGAGGAGACCATGTG-3' (forward) and 5'-GGGCTTCTTGGAGAAGAT-3' (reverse); *PTCH1*, 5'-CCACAGAAGCGCTCCTACA-3' (forward) and 5'-CTGTAATTTGCCCCCTTCC-3' (reverse); *PTCH2*, 5'-GGAATGATTGAGCGGATGATTGA-3' (forward) and 5'-CCACCTGTGCCTTGTCTAGC-3' (reverse); *PTCHD1*, 5'-AGCACCGTCTCTACTCGGAC-3' (forward) and 5'-GAACCTGGATCTTGGTGACAG-3' (reverse); *PTCHD2*, 5'-GCTGGGCTCCTACTCCTACT-3' (forward) and 5'-GGGGTGTCCAAACAGGAT-3' (reverse); *PTCHD3*, 5'-ACCTAGAGGAGCATTACCCC-3' (forward) and 5'-GAAGCGGTAGGAGTCGTTGG-3' (reverse); *NPC1*, 5'-GTCTCCGAGTACTCCTCCATC-3' (forward) and 5'-CGCAGTAATGAAGACCAGCGA-3' (reverse); *GLI1*, 5'-CCACGGGGAGCGGAAGGAG-3' (forward) and 5'-ACTGGCATTGCTGAAGGCTTTACTG-3' (reverse).

**Luciferase Assays**—The putative *PTCH53* binding sites BS1 and BS2 were amplified and cloned upstream of the luciferase reporter in pBV-Luc (Addgene plasmid 16539). DLD-1 cells growing on 12-well plates were co-transfected with firefly luciferase reporter plasmids, the pGL4.74 *Renilla* luciferase

reporter construct (Promega), and pCMV-p53 (wild type; Addgene 16434) or pCMV-p53 R175H (Addgene 16436). Lysates were collected 24 h after transfection with Lipofectamine 2000 (Life Technologies). For the assessment of the effects of Patched proteins on SMO activity, C3H10T1/2 cells or *Smo*<sup>-/-</sup> mouse embryo fibroblasts were transfected with 200 ng Gliuciferase reporter plasmid, 200 ng of pGL4.74, 150 ng of SMO expression plasmid, and varying mass ratios of *PTCH1*, *PTCHD1*, or *PTCH53* expression plasmids. Transfected cells were split into three wells 8 h after transfection. After 24 h, medium was replaced with DMEM containing reduced serum (0.5% FBS). Lysates were collected 72 h after transfection. Firefly luciferase and *Renilla* luciferase activity was determined using the Dual-Luciferase reporter assay system (Promega) with the Victor3 plate reader (PerkinElmer Life Sciences). Firefly luciferase readings were normalized to *Renilla* luciferase to correct for transfection efficiency. All experiments were performed in triplicate with at least three independent experiments.

**Cell Line and Tumor Database Analysis**—*TP53* mutations in diverse cell lines were extracted from the database maintained by the Sanger Cell Lines Project (11) and the Cancer Cell Line Encyclopedia maintained by the Broad Institute (12); gene expression data were also extracted from the Cancer Cell Line Encyclopedia. Mutation and gene expression data from tumors assembled in the Cancer Genome Atlas were extracted via cBioPortal (13). The relative expression of each queried gene in *TP53* wild type and *TP53* mutant sample sets is indicated by a z-score, a dimensionless value that represents the number of S.D. values by which expression differs from the mean of all measured transcripts in each reference population.

**Statistical Analyses**—Student's two-tailed *t* tests were used to assess significance: \*,  $p < 0.05$ ; \*\*,  $p < 0.02$ ; \*\*\*,  $p < 0.005$ . Error bars indicate S.E.

**Lentiviruses, Gene Induction, and Knockdown**—A full-length *PTCH53* cDNA was cloned into the expression vector pcDNA3.1 (Invitrogen) and subcloned into the lentivector pLVX-mCherry (Clontech) and the doxycycline-inducible lentivector pINDUCER20 (14). For inducible knockdown of *PTCH53*, an shRNA cassette encoded by the sense sequence 5'-CGAGCCGTGCTGGAAATGA-3' was cloned into the lentivector pINDUCER10 (14). Lentiviruses were generated by co-transfecting shRNA- or cDNA-expressing lentiviral vectors with packaging plasmids pMD2.G (Addgene plasmid 12259) and pSPAX2 (Addgene plasmid 12260) into 293T cells using Eugene HD (Promega). Viral supernatants were harvested 48 h after transfection and filtered through 0.45- $\mu$ m filters (Corning, Inc.). For cell lines stably harboring inducible pINDUCER elements (14), expression was induced by 1  $\mu$ g/ml doxycycline.

**Hedgehog Pathway Activity Analysis**—For generation of conditioned media, 293T cells were transfected with pcDNA3-SHH-N, with Eugene HD (Promega). Control conditioned media from mock-transfected 293T cells or ShhN-conditioned media were collected 48 h after transfection and filtered through 0.45  $\mu$ m filters. Cells were incubated for 24 h in medium with reduced serum (0.25% FBS). Conditioned media were added at a 1:5–1:20 dilution. Where indicated, purmor-

## p53 Activates a PTCH1 Homolog

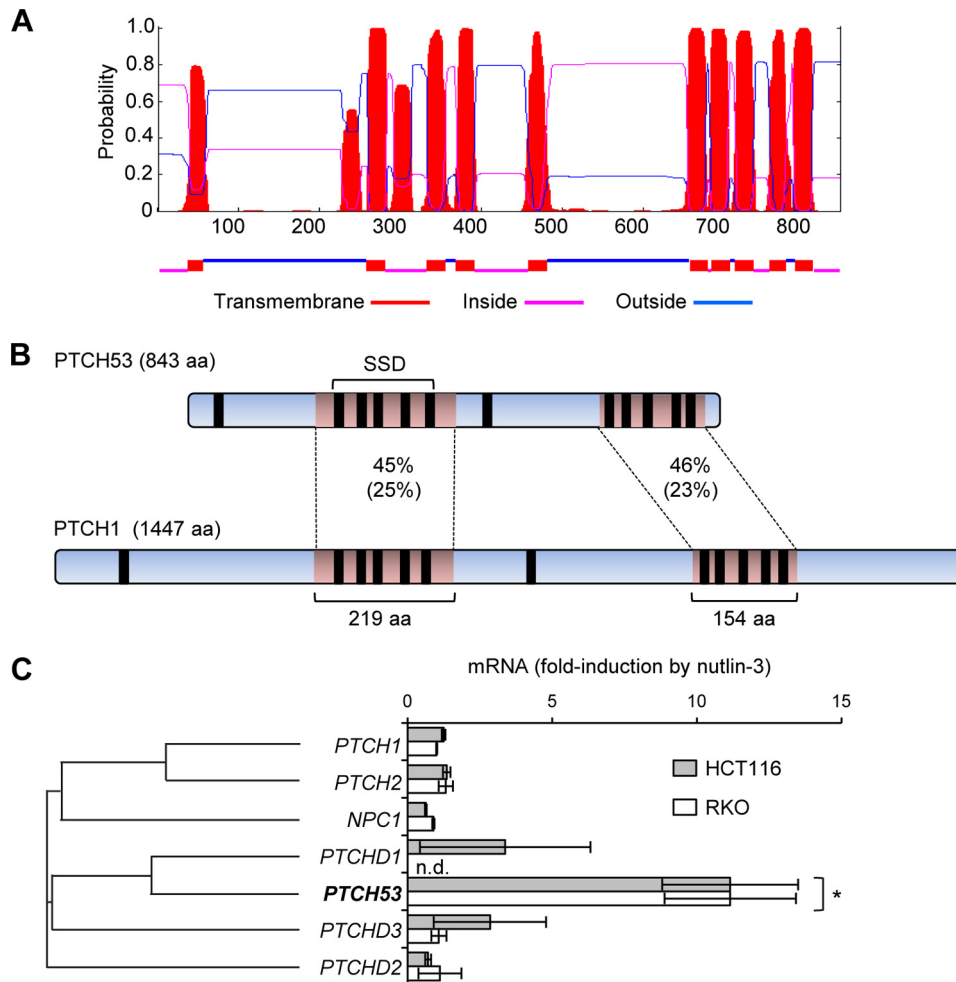


**FIGURE 1. A human Patched gene is expressed in cells that harbor wild type TP53.** *A*, predicted topology of the transmembrane domains of the *PTCH53*-encoded protein, as predicted by a hidden Markov model (35), assuming an interior C terminus. *B*, alignment of the predicted *PTCH53* protein (843 amino acid residues) and *PTCH1* (1447 amino acid residues). The two characteristic regions of homology shared by Patched proteins are shaded in orange. Black bars, transmembrane domains. SSD, sterol-sensing domain. The amino acid similarity within each region is indicated as a percentage; the percentage of identical amino acids is shown in parentheses. *C*, HCT116 and RKO cells were treated for 24 h with DMSO or 10  $\mu$ M nutlin-3. The expression of human Patched genes, shown in the order of their positions on a phylogenetic tree, was quantified by qPCR. Relative gene induction by nutlin-3 is normalized to expression after DMSO treatment (\*,  $p < 0.05$ ).  $n \geq 3$  independent experiments. n.d., not detected. Error bars, S.E.

phamine (Sigma-Aldrich) was added to a final concentration of 10  $\mu$ M.

## RESULTS

*A Homolog of PTCH1 Is Commonly Down-regulated in TP53 Mutant Colorectal Cancer Cells*—To identify novel, high confidence p53 target genes, we evaluated transcripts that were differentially expressed in isogenic colorectal cancer cell lines harboring mutant or wild type *TP53*. The wild type *TP53* alleles in HCT116, RKO, and SW48 had previously been knocked out by recombinant adeno-associated virus-mediated gene targeting; the *TP53* mutation harbored by DLD-1 cells had been reverted to wild type by a knock-in approach (10). A total of 21 genes were up-regulated at least 2-fold by ionizing radiation in a p53-dependent manner in each of these four isogenic cell pairs (10). One commonly p53-regulated probe was found to map to the uncharacterized gene *C6ORF138*. Transcripts from this locus encode a hypothetical protein with transmembrane domains that are associated with members of the Patched family. *C6ORF138* had therefore been assigned the alternative des-

ignation *PTCHD4*. In light of the homology of this previously uncharacterized gene to members of the human Patched family and its possible regulation by p53, we hereafter refer to this gene as *PTCH53*.

The Patched proteins are characterized by 12-transmembrane domains and feature a sterol-sensing motif and a second region that encompasses five additional transmembrane domains near the C terminus. This structural arrangement, first observed in the Patched protein encoded by *Drosophila*, is evolutionarily conserved (15). In humans, the prototypical Patched protein is encoded by *PTCH1*, a tumor suppressor that functions as the primary negative regulator of Hedgehog signaling. The predicted protein encoded by *PTCH53* conformed to the general structure of the Patched proteins (Fig. 1*A*) and was found to share significant homology with *PTCH1* in the two conserved regions (Fig. 1*B*). Alignment of the two protein sequences revealed a 219-amino acid block of homology around the sterol-sensing domain of *PTCH1*. In this region, 45% of the amino acids were in similar functional groups, and 25% were identical, with five gaps (2%). A 154-amino acid



region of homology spanning the C-terminal transmembrane domain cluster was 46% similar and 23% identical, with 14 gaps (9%). Among the human *Patched* orthologs, only *PTCH53* was induced in a p53-dependent manner by nutlin-3 (Fig. 1C), a drug that stabilizes and activates p53 by inhibiting the HDM2 ubiquitin ligase.

*The Transcription of PTCH53 Is Directly Controlled by p53*—To rigorously confirm the role of p53 in the transcriptional regulation of *PTCH53*, we first measured gene expression by quantitative reverse transcription PCR (qPCR) in HCT116, RKO, and SW48 cells and in their respective *TP53*-knock-out derivatives. In this panel of colorectal cancer cells, *PTCH53* transcripts were more abundant in *TP53*<sup>+/+</sup> cells compared with isogenic *TP53*<sup>-/-</sup> cells. Incubation with nutlin-3 caused a *TP53* genotype-dependent increase in *PTCH53* expression in each cell pair (Fig. 2A). The ~10-fold induction of *PTCH53* in *TP53* wild type cells was comparable in magnitude to the extensively studied p53 target gene *CDKN1A* (alternatively known as *p21*) in all three cell pairs. *PTCH53* expression was similarly induced in a *TP53*-dependent manner when these cells were exposed to  $\gamma$ -irradiation, a potent stimulus of p53 activation (Fig. 2B).

The abundance of *PTCH53* transcripts was low in DLD-1 cells, which harbor a *TP53* S241F mutation and express no wild type p53 (Fig. 2C). A derivative of DLD-1 in which this endogenous mutation had been repaired (10) exhibited up-regulation of both *PTCH53* and *CDKN1A* (Fig. 2C). *PTCH53* was similarly responsive to nutlin-3 in non-cancer cells, including diploid human fibroblasts derived from colon (Ccd-18Co) and lung (IMR90) (Fig. 2D). The kinetics of *PTCH53* induction after treatment with nutlin-3 (Fig. 2E) and the magnitude of *PTCH53* induction in response to increasing doses of ionizing radiation (Fig. 2F) were comparable with those of *CDKN1A* in HCT116 cells that harbor intact, wild type *TP53* alleles.

Direct p53 target genes are regulated through binding of the p53 tetramer to bipartite 20-bp sites conforming to the half-site consensus sequence RRRCCWGGYYY (16). We used the p53MH algorithm (17) to identify potential p53 binding sites in the vicinity of the *PTCH53* locus. The nearest 20/20 match was located 42 kb upstream of the 5' exon of *PTCHD4*, as annotated in GenBank<sup>TM</sup> (Fig. 3A). We employed the rapid amplification of cDNA ends (RACE) method to determine whether additional upstream exons were located nearer to this putative binding site. Amplified cDNA products were sequenced and aligned to the human genome with the UCSC Human Genome Browser (18). Two upstream exons were identified that were not included in the annotated *PTCHD4* gene (Fig. 3A). RNAseq data from the Encyclopedia of DNA Elements (ENCODE) project (19) indicated that the *PTCH53* exon adjacent to the putative p53 binding site was actively transcribed (Fig. 3B). Furthermore, ENCODE data from this region exhibited DNase I hypersensitivity and expression of the chromatin marks H3K4Me3, H3K27Ac, and H3K4Me1, a pattern of epigenetic modifications that is consistent with an active promoter enhancer region (19) (Fig. 3B).

The putative start of transcription was positioned 22 bp downstream of the identified p53 binding site (Fig. 3A). When cloned into a luciferase reporter construct, this site (BS1) con-

ferred responsiveness to wild type p53 but not to the cancer-associated R175H mutant (Fig. 3C). In contrast, a second putative binding site (BS2) located between exons 2 and 3 that matched the p53 consensus at 14 of 20 positions (Fig. 3A) was not p53-responsive (Fig. 3C). A direct, inducible interaction between p53 and the BS1 site was detected by chromatin immunoprecipitation. Binding of p53 to this site could be detected in untreated cells and was increased following treatment with nutlin-3 or ionizing radiation (IR; Fig. 3D). The inducible interaction between p53 and the *PTCH53* element was similar to the interaction between p53 and the binding site previously identified in the *CDKN1A* locus (5). In contrast, no interaction was detected at the degenerate BS2 site (Fig. 3D). These results suggest that *PTCH53* is a direct transcriptional target of p53.

*PTCH53 Expression Is Associated with TP53 Status in Diverse Tumor Types*—We next asked whether *PTCH53* expression was related to *TP53* status in larger panels of cell lines and tumors. Global gene expression data and *TP53* genotype status were available for 1036 cell lines characterized in the Cancer Cell Line Encyclopedia (12). In this extensive data set, *PTCH53* was expressed at significantly lower levels in cell lines harboring *TP53* mutations, as was the prototypic p53 target gene *CDKN1A* (Fig. 4A). The dependence of *PTCH53* expression on functional p53 was most apparent and highly statistically significant in cell lines derived from tumors in the central nervous system and skin (Fig. 4B) and could be observed in other tissues as well.

*TP53* is the most frequently mutated gene in 12 types of cancer extensively profiled in the Cancer Genome Atlas. Of more than 3000 annotated tumors, 42% harbor a *TP53* mutation (20). Comprehensive mutational and expression data were available for melanomas, glioblastomas, colorectal cancers, and breast cancers. In each of these four tumor types, *PTCH53* and *CDKN1A* were both expressed at relatively high levels in tumors that retained wild type *TP53* (Fig. 4C). Such a clear *TP53* genotype-dependent pattern of expression in multiple cancer types was not observed for many other genes that have been demonstrated to be responsive to p53 *in vitro* (Fig. 5) Among the 80 previously identified and experimentally validated p53 targets that we queried in this fashion, only six genes, *PTCH53*, *CDKN1A*, *DDB2*, *CCNG1*, *RP27L*, and *FDXR*, were differentially expressed at a high degree of significance ( $p < 0.01$ ) in *TP53* wild type and *TP53* mutant tumors in all four tumor types (Fig. 5 and Table 1). Forty-eight genes were more highly expressed ( $p < 0.01$ ) in *TP53* wild type tumors from at least one of the four types of cancer; 11 genes were differentially expressed in one or more tumor types at lower levels of significance ( $p < 0.05$ ). Of the 80 genes queried, 21 were not differentially expressed in any of the four tumor types ( $p > 0.05$ ) (Table 1).

*PTCH53 Inhibits Canonical Hedgehog Signaling*—PTCH1 potently represses human Hh signaling by counteracting the activity of the seven-transmembrane G protein-coupled receptor SMO. In this canonical Hh pathway, the binding of a Hh ligand by PTCH1 relieves the repression of SMO and results in the downstream activation of the GLI family of transcription factors (21). Hh signaling is repressed in most adult tissues, but mutations in *PTCH1*, *SMO*, or the downstream mediator

## p53 Activates a PTCH1 Homolog

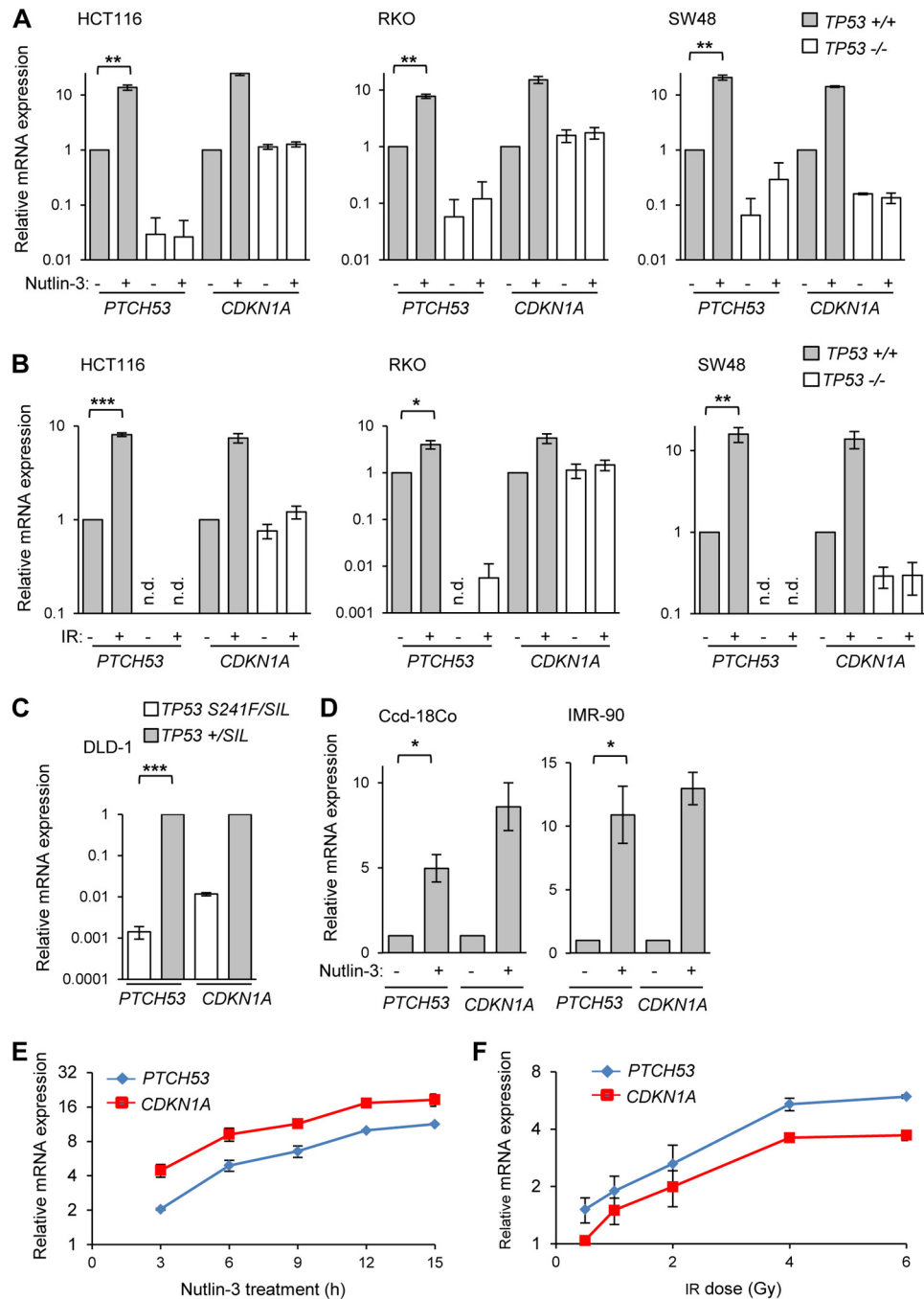


**FIGURE 2. Expression of *PTCH53* is dependent on *TP53* genotype.** *A*, a panel of isogenic colorectal cancer cell pairs (genotype  $TP53^{+/+}$  or  $TP53^{-/-}$ ) were treated with  $10 \mu\text{M}$  nutlin-3 for 24 h, as indicated. *PTCH53* and *CDKN1A* transcripts were assessed by qPCR.  $n > 3$  independent experiments. *B*, expression of *PTCH53* and *CDKN1A* was assessed 24 h after cells were exposed to ionizing radiation (IR; 12 grays). *C*, *PTCH53* and *CDKN1A* transcripts were assessed by qPCR in DLD-1 cells (genotype  $TP53^{S241F/SIL}$ ) and in an isogenic derivative with restored wild type p53 function ( $TP53^{+/SIL}$ ).  $n = 4$  independent experiments. *D*, expression of *PTCH53* and *CDKN1A* in fibroblast cell lines Ccd-18Co and IMR-90, before and after treatment with  $10 \mu\text{M}$  nutlin-3 for 24 h, as indicated.  $n = 2$  independent experiments. HCT116 ( $TP53^{+/+}$ ) cells were treated with  $10 \mu\text{M}$  nutlin-3 and harvested at the indicated times (*E*) or treated with the indicated doses of ionizing radiation and harvested after 24 h (*F*). Induction of transcription at *PTCH53* and *CDKN1A* was measured by qPCR.  $n = 2$  independent experiments. *n.d.*, not detected. Error bars, S.E.

encoded by *SUFU* cause constitutive, ligand-independent activation of Hh signaling in cancers (22). Driver mutations in these genes are typically found in basal cell carcinomas and Shh subtype medulloblastomas and have been detected in other cancers at much lower frequency (23). Most cancers with evidence of activated Hh signaling do not harbor a mutation in any of the genes known to populate the canonical Hh pathway.

We tested whether *PTCH53* could function as a negative regulator of canonical Hh signaling. The effect of *PTCH53* expression was first examined in the medulloblastoma cell line DAOY, which exhibits the transcriptional signature of the Shh subtype (24). Unlike the vast majority of cancer-derived cell lines maintained in culture (25), DAOY cells retain the ability to up-regulate Hh signaling in response to ligand or drugs that can acti-

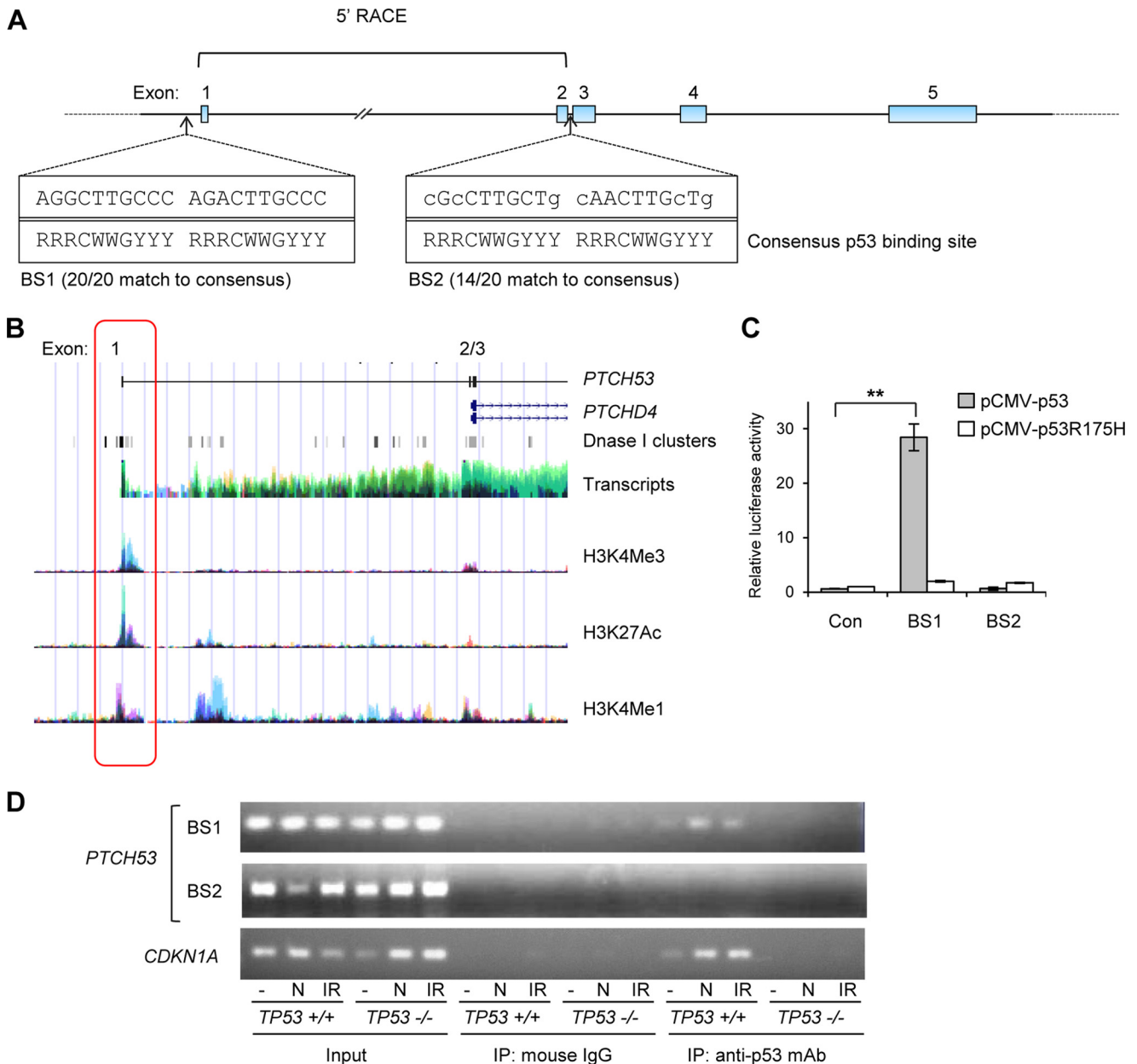


**FIGURE 3. p53 directly regulates the *PTCH53* promoter.** *A*, genomic structure of *PTCH53*. Exons 1 and 2 were newly identified by 5'-RACE. A putative p53 binding site (BS1) was located 22 bp upstream of the first exon. A second partial site (BS2) located between exons 2 and 3 was a 14/20 match with the consensus sequence. *B*, regions of active transcription, as assessed by RNA-Seq on nine cell lines, and DNase sensitivity and activating histone marks from seven cell lines (19) were overlaid onto the upstream exons of *PTCH53* and the previously identified *PTCHD4* exons. The newly identified exon 1 is within the region circled in red. *C*, putative p53 binding sites BS1 and BS2 were cloned upstream of a luciferase reporter plasmid. These plasmids or the empty vector (*Con*) were co-transfected with plasmids that express wild type *TP53* or the R175H mutant into *TP53* mutant DLD-1 cells. *Renilla* luciferase activity was used to normalize transfection efficiency. *n* = 3 independent experiments. *D*, *TP53*<sup>+/+</sup> and *TP53*<sup>-/-</sup> HCT116 cells were untreated (-) or treated with 10  $\mu$ M nutlin-3 (*N*) or 12-gray ionizing radiation (*IR*) and harvested 24 h later. Chromatin immunoprecipitation (*IP*) was performed using control mouse IgG or anti-p53 mouse monoclonal antibody. The BS1 and BS2 sites in *PTCH53* and the p53 binding site in the *CDKN1A* promoter were amplified by PCR from input DNA and from immunoprecipitated DNA templates. Error bars, S.E.

vate SMO activity (26). Lentiviral delivery of a *PTCH53* transgene to DAOY cells caused down-regulated basal expression of the Hh target genes *GLI1*, *PTCH1*, and *PTCH2* and attenuated the responses of these genes to processed ligand (ShhN) and the SMO agonist purmorphamine (Fig. 6A).

We next used a luciferase reporter oriented downstream of eight Gli binding sites (Gli-luc) to measure the cumulative effects of SMO on transcriptional activity by the GLI proteins (27). Transfection of a SMO expression plasmid into *Smo*<sup>-/-</sup>

mouse embryonic fibroblasts activated the co-transfected Gli-luc reporter, as expected (Fig. 6B). The activation of the Gli-luc reporter by exogenous SMO could be inhibited by co-transfection with a *PTCH53* expression plasmid; the extent of inhibition was related to the amount of plasmid transfected. Similar results were obtained in the Shh-responsive murine cell line C3H10T1/2 (Fig. 6C), which is routinely employed for functional analysis of the canonical Hh pathway. Expression of *PTCH53*, *PTCHD1*, and *PTCH1* each inhibited basal (unstimu-

## p53 Activates a PTCH1 Homolog

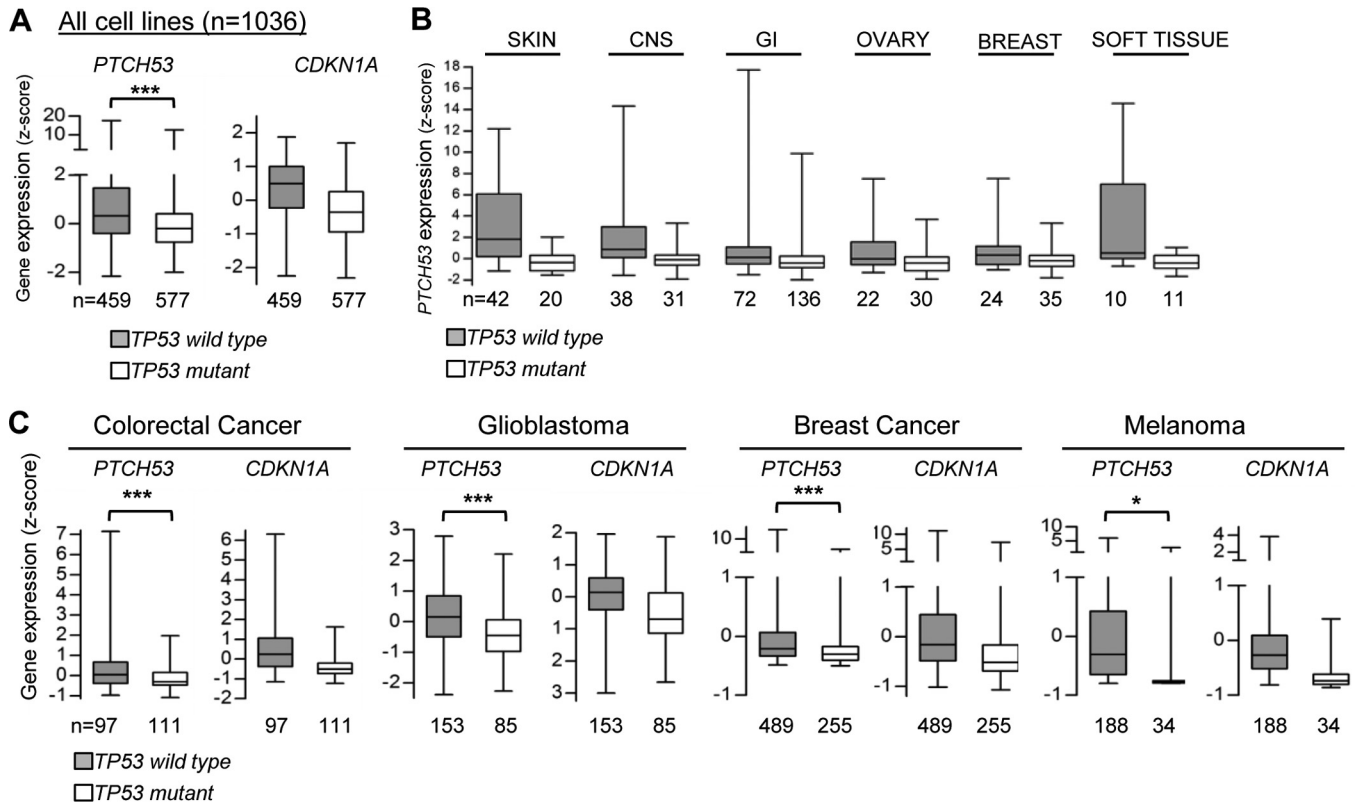


FIGURE 4. Gene expression and *TP53* status in cancer cell lines and tumors. A, relative expression of *PTCH53* and *CDKN1A* RNAs in *TP53* wild type ( $n = 459$ ) and *TP53* mutant ( $n = 577$ ) cell lines comprehensively characterized in the Cancer Cell Line Encyclopedia (12). \*\*\*,  $p < 0.0001$ . B, differential expression of *PTCH53* in *TP53* wild type and mutant cell lines derived from skin ( $p = 1.4 \times 10^{-4}$ ), central nervous system (CNS;  $p = 9.2 \times 10^{-4}$ ), gastrointestinal (GI;  $p = 1.2 \times 10^{-3}$ ), ovarian ( $p = 1.2 \times 10^{-3}$ ), breast ( $p = 1.3 \times 10^{-2}$ ), and soft tissue tumors ( $p = 4.8 \times 10^{-2}$ ). C, relative expression of *PTCH53* and *CDKN1A* RNAs in *TP53* wild type or *TP53* mutant human tumors from the Cancer Genome Atlas. \*\*\*,  $p < 0.0001$ ; \*,  $p < 0.01$ . Error bars, S.E.

lated) Hh signaling and also inhibited reporter activity stimulated by expression of exogenous SMO (Fig. 6C). Among these homologous genes, *PTCH1* was the most potent inhibitor of Gli-luciferase activation; inhibition was apparent even when *PTCH1* plasmid was delivered at a low mass ratio (Fig. 6, B and C). These results suggest that *PTCH53* can act as a suppressor of canonical Hh signaling by antagonizing the effects of SMO, to an extent that was similar to the evolutionarily related *PTCHD1*. In the absence of acute stimulation of the p53-PTCH53 pathway, no correlation between the expression of *GLI1* and *PTCH53* was observed in diverse cell lines or tumor samples (data not shown).

To begin to evaluate an upstream role for p53 in the regulation of Hh signaling, we tested whether nutlin-3 treatment could cause the suppression of Hh activity in human cells with wild type *TP53*. Stimulation of p53-mediated transcription by nutlin-3 caused increased expression of *PTCH53* and *CDKN1A*, as expected, and decreased expression of the canonical Hh target genes *GLI1*, *PTCH1*, and *PTCH2* in normal human colon fibroblast cells with basally active Hh signaling and cells in which Hh activity was stimulated by ShhN ligand (Fig. 7A). The immortalized retinal epithelial cell line hTERT-RPE1 also retains an intact Hh signaling pathway, as evidenced by the increased expression of *GLI1* in response to ShhN ligand (Fig. 7B). We transduced these non-cancer cells with a doxycycline-inducible *PTCH53* expression system based on the pINDUCER lentivirus (14). Induction of *PTCH53* expression

caused down-regulation of *GLI1* expression, both in the absence and presence of Shh ligand (Fig. 7C). *GLI1* expression was similarly down-regulated in this *TP53* wild type cell line following nutlin-3 treatment (Fig. 7D).

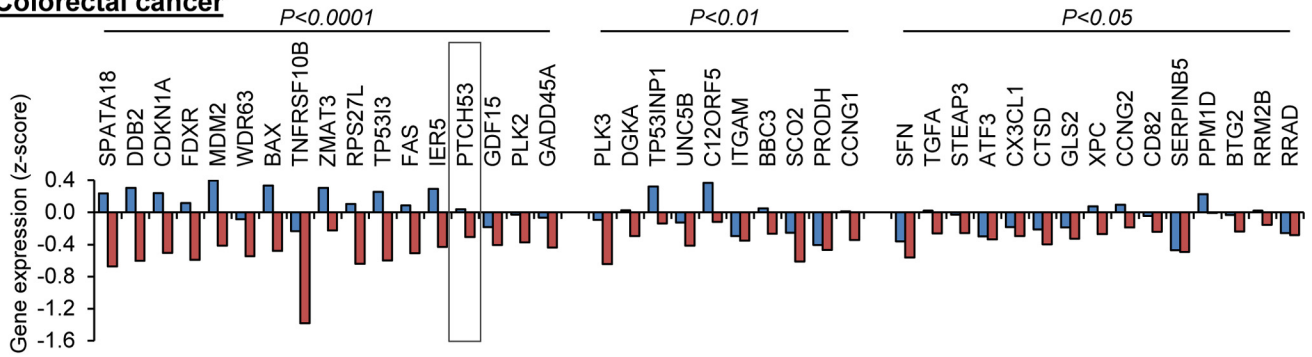
In isogenic cell pairs, a significant down-regulation of *GLI1* in response to nutlin-3 was only observed in cells that retained wild type *TP53* alleles (Fig. 7E), confirming that the repression of Hh signaling in response to nutlin-3 was mediated by p53. To determine whether this function required the up-regulation of *PTCH53*, we derived *TP53* wild type, Hh-responsive cell lines that expressed an inducible shRNA. The induction of the best *PTCH53*-targeted shRNA in untreated hTERT-RPE1 and CCD18-Co cells reduced *PTCH53* expression to about 40% of the basal level (Fig. 7, F and G). In cells treated with nutlin-3, *PTCH53* could be knocked down to the basal level that was observed in untreated cells. The knockdown of *PTCH53* to these intermediate levels had no significant effect on *GLI1* expression in either cell line (Fig. 7, F and G). These results suggest that, in these experimental systems, *PTCH53* was not required for the efficient repression of canonical Hh activity by stabilized p53.

## DISCUSSION

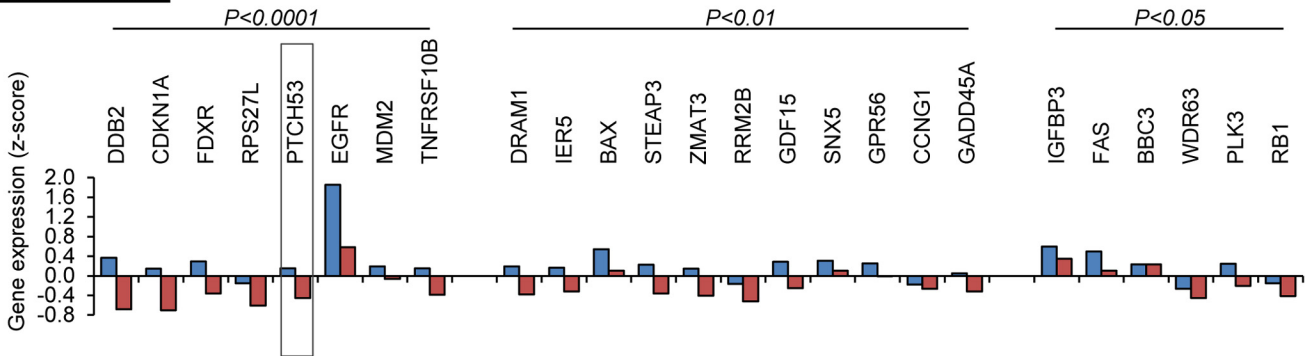
A large number of genes can be activated by p53, and an even larger number of p53 binding sites are located throughout the human genome. This multitude of targets has made it challenging to fully understand how mutations in *TP53* promote tumor-



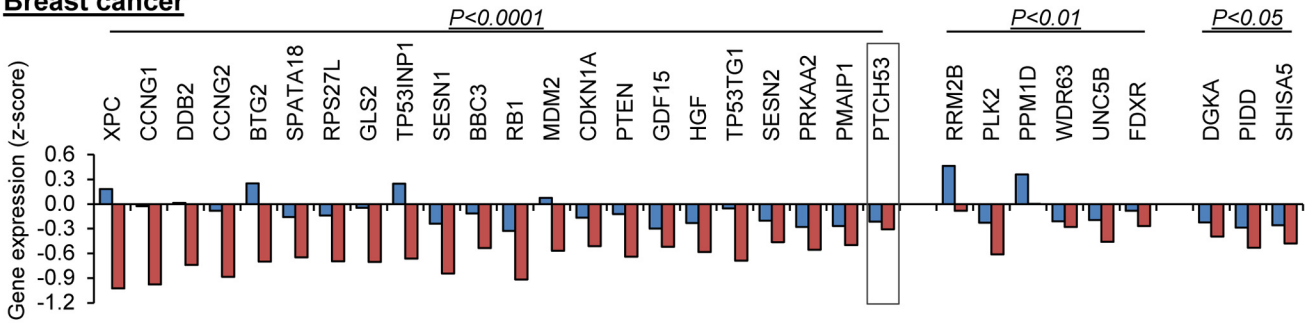
**Colorectal cancer**



**Glioblastoma**



**Breast cancer**



**Melanoma**

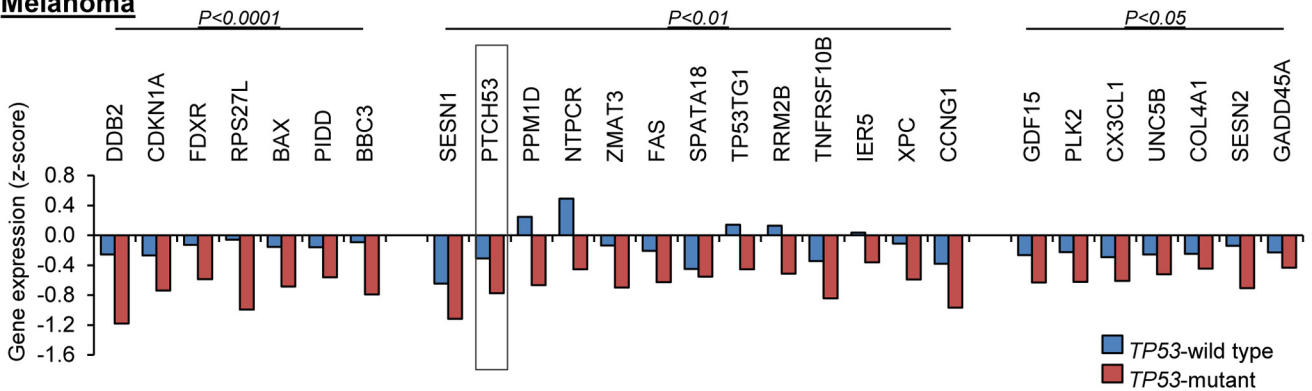


FIGURE 5. **Expression of p53 target genes in *TP53* wild type and *TP53* mutant tumors.** Expression values of 80 p53 target genes (Table 1) were examined in colorectal cancers, gliomas, breast cancers, and melanomas annotated in the Cancer Genome Atlas (20). The median gene expression value (z-score) for each target gene in *TP53* wild type (blue bars) and *TP53* mutant (red bars) tumor samples is shown. Genes are ranked in order of *p* value.

igenesis in diverse tissues. A recent analysis of large panels of molecularly characterized tumors has suggested that relatively few genes are consistently expressed at higher levels in tumors

that retain wild type *TP53* (8). Our analysis confirms that the genes most commonly and most robustly regulated by p53 predominantly function in pathways that regulate the cell cycle,



## p53 Activates a PTCH1 Homolog

**TABLE 1**

p53 target genes queried in TCGA data sets (n = 80)

Differential expression in four cancers <sup>a</sup>							
4/4	<i>CCNG1</i>	<i>CDKN1A</i>	<i>DDB2</i>	<i>FDXR</i>	<i>PTCH53</i>	<i>RPS27L</i>	
3/4	<i>BAX</i>	<i>BBC3</i>	<i>GDF15</i>	<i>IER5</i>	<i>MDM2</i>	<i>SPATA18</i>	<i>ZMAT3</i>
2/4	<i>FAS</i>	<i>GADD45A</i>	<i>PLK2</i>	<i>PPM1D</i>	<i>RRM2B</i>	<i>SESN1</i>	<i>TLR3</i>
	<i>TNFRSF10B</i>	<i>TP53INP</i>	<i>TP53TG1</i>	<i>UNC5B</i>	<i>WDR63</i>	<i>XPC</i>	
1/4	<i>BTG2</i>	<i>C12ORF5</i>	<i>CCNG2</i>	<i>DGKA</i>	<i>DRAM1</i>	<i>EGFR</i>	<i>GLS2</i>
	<i>GPR56</i>	<i>HGF</i>	<i>ITGAM</i>	<i>NTPCR</i>	<i>PIDD</i>	<i>PLK3</i>	<i>PMAIP1</i>
	<i>PRKAA2</i>	<i>PRODH</i>	<i>PTEN</i>	<i>RB1</i>	<i>SCO2</i>	<i>SESN2</i>	<i>SNX5</i>
	<i>STEAP3</i>	<i>TP53I3</i>					
0/4	<i>ATF3</i>	<i>BDKRB2</i>	<i>CD82</i>	<i>COL4A1</i>	<i>CTSD</i>	<i>CX3CL1</i>	<i>DKK1</i>
	<i>EIF2AK2</i>	<i>GML</i>	<i>GPC3</i>	<i>GTSE1</i>	<i>IGFBP3</i>	<i>MET</i>	<i>MMP2</i>
	<i>MYBL1</i>	<i>P2RX6</i>	<i>PCBP4</i>	<i>PCNA</i>	<i>PTP4A3</i>	<i>RPRM</i>	<i>RRAD</i>
	<i>S100A2</i>	<i>SERPINE5</i>	<i>SERPINE1</i>	<i>SFN</i>	<i>SHISA5</i>	<i>STAU1</i>	<i>TAP1</i>
	<i>TGFA</i>	<i>TSC2</i>	<i>YBX3</i>				

<sup>a</sup> Decreased expression in *TP53* mutant tumors from TCGA colorectal cancer, breast cancer, glioma, and melanoma data sets,  $p < 0.01$ .

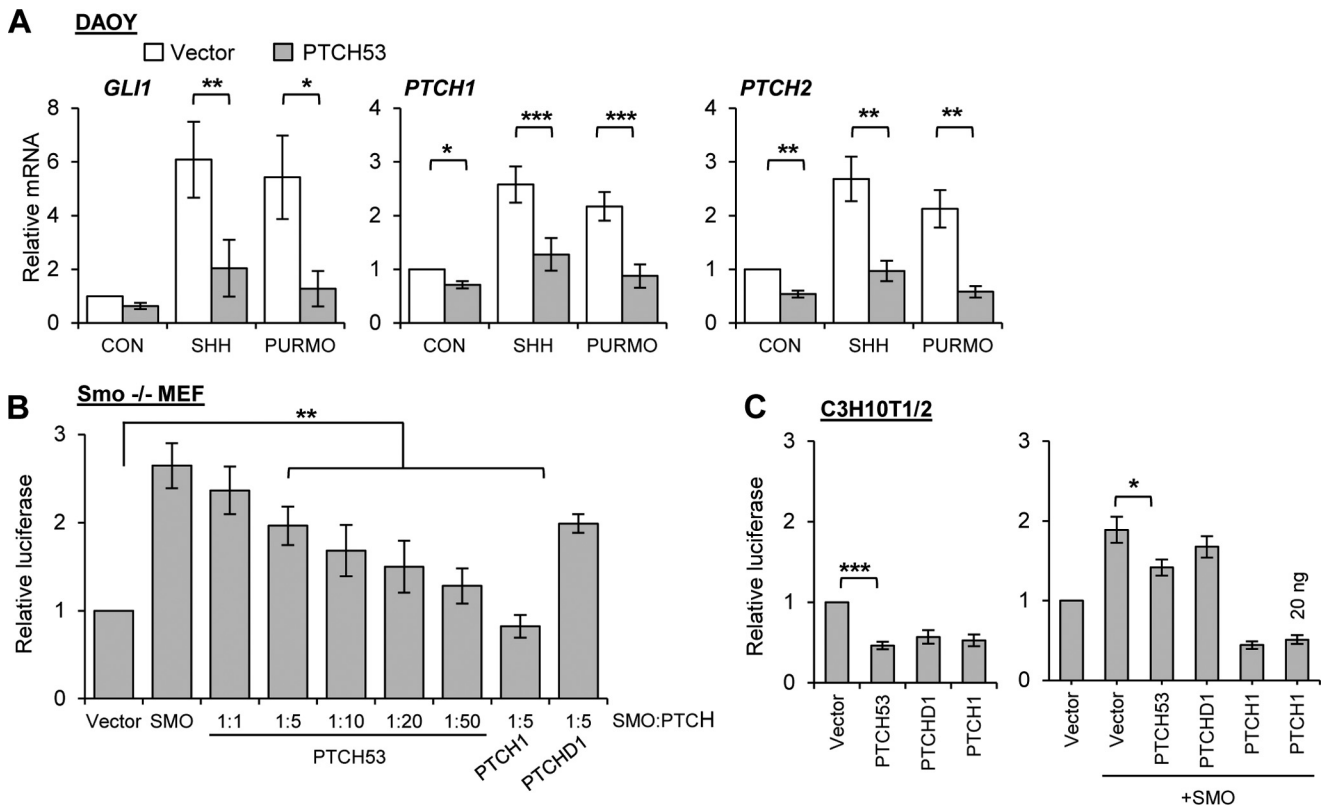


**FIGURE 6. Inhibition of canonical Hh signaling by *PTCH53*.** **A**, DAOY medulloblastoma cells were infected with a *PTCH53* expression lentivirus or empty vector and subsequently treated with control conditioned medium (Con), Shh-conditioned medium (SHH), or the SMO agonist purmorphamine (PURMO; 10  $\mu$ M) for 24 h. Expression of the Hh target genes *GLI1*, *PTCH1*, and *PTCH2* was assessed by qPCR.  $n = 4$  independent experiments. **B**, *Smo<sup>-/-</sup>* mouse embryonic fibroblasts were co-transfected with a *SMO* expression plasmid, a Gli-luciferase reporter, and plasmids that direct the expression of *PTCH53*, *PTCH1*, or *PTCHD1* at the indicated mass ratios (SMO/PTCH). Luciferase activity was assessed 72 h after transfection. *Renilla* luciferase activity was used to normalize transfection efficiency.  $n > 3$  replicates. **C**, C3H10T1/2 cells were co-transfected with the Gli-luc reporter and plasmids that direct the expression of *PTCH53*, *PTCH1*, or *PTCHD1* (300 ng of plasmid DNA/transfection) and SMO (60 ng of plasmid DNA/transfection), as indicated. Luciferase levels were measured 24 h after transfection.  $n = 6$  independent experiments. Error bars, S.E.

facilitate DNA repair, and mediate cell death. Many other genes appear to be induced by p53 at lower levels and in a cell type- or tissue-specific fashion. Possibly, such genes have more specialized functions. It is also possible that some of the p53-responsive genes that are important for tumor suppression may not require high levels of induction. Such genes would be inherently difficult to identify by the data mining approaches employed here.

In this study, we show that a previously uncharacterized homolog of *PTCH1* is one of a small number of human genes

whose expression is most strongly associated with *TP53* genotype. This widespread, p53-dependent pattern of expression suggests that *PTCH53* might play a fundamental role in tumor suppression. Although *PTCH1* is a well characterized tumor suppressor gene, the functions of the human *PTCH1* homologs and their potential roles in cancer have remained obscure.

What is the physiological role of *PTCH53*? Our data demonstrate that *PTCH53* is highly responsive to p53 and is therefore a component of the DNA damage response. Unique among the human Patched genes, *PTCH53* apparently functions as a

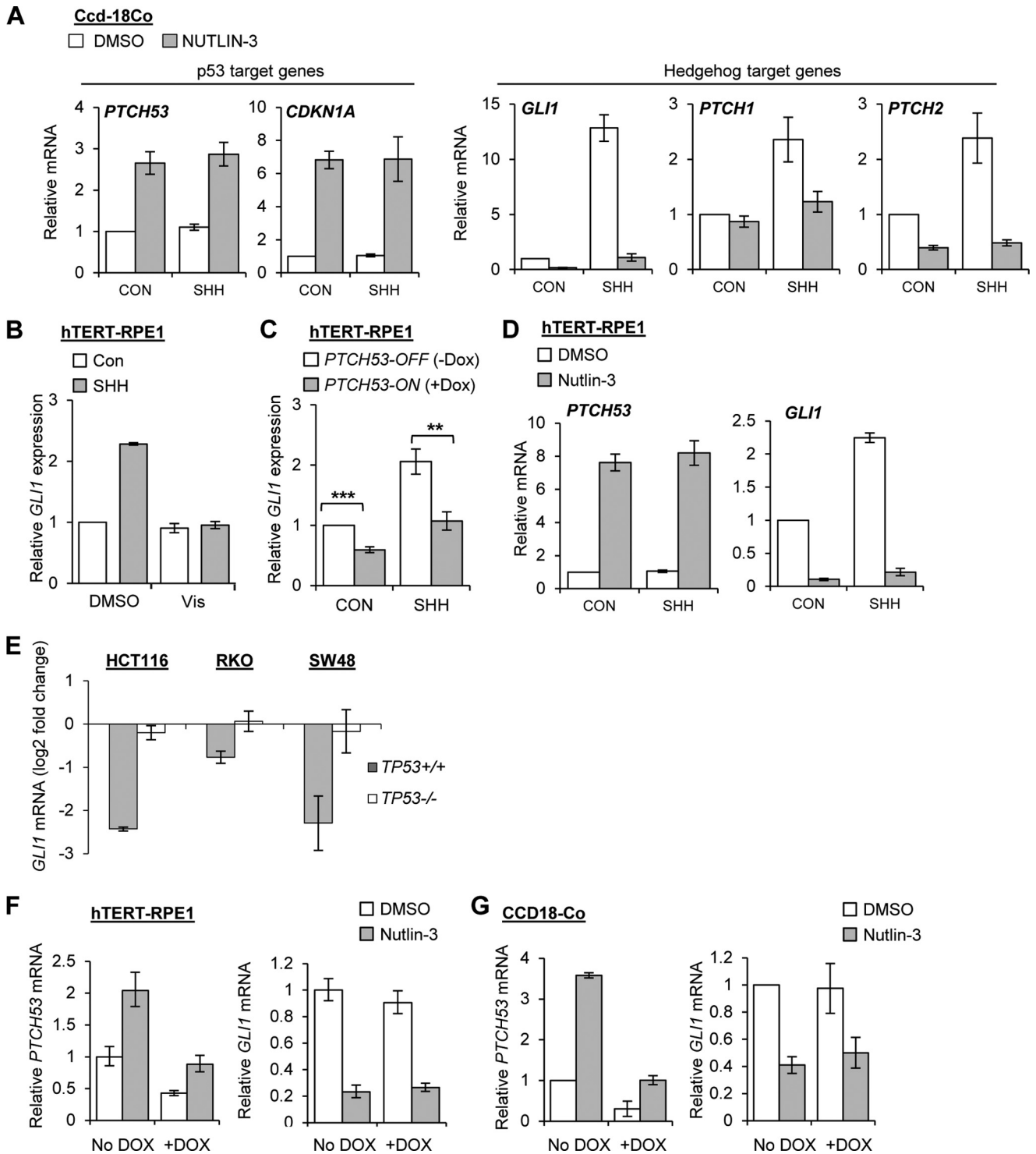


**FIGURE 7. Repression of canonical Hh signals by p53.** *A*, Ccd-18Co cells were treated with DMSO or 10  $\mu$ M nutlin-3 for 24 h in control conditioned medium (Con) or SHH-conditioned medium (SHH). Expression of *PTCH53*, *CDKN1A*, *GLI1*, *PTCH1*, and *PTCH2* was assessed by qPCR. *n* = 3 independent experiments. *B*, hTERT-RPE1 cells were incubated in SHH-conditioned medium or control medium (Con) for 72 h and then treated with DMSO or 0.2  $\mu$ M vismodegib (Vis) for 48 h. DMSO or Nutlin-3 was then added for an additional 24 h. *GLI1* expression was measured by qPCR. *n* = 3 independent experiments. *C*, hTERT-RPE1 cells with doxycycline-inducible *PTCH53* were stimulated with Shh ligand for 24 h and then treated with or without doxycycline for 48 h to induce *PTCH53* expression. *GLI1* expression was assessed by qPCR. *n* = 6 independent experiments. *D*, hTERT-RPE1 cells were stimulated with Shh ligand for 24 h and were then treated with DMSO or 10  $\mu$ M nutlin-3 for 24 h. *PTCH53* and *GLI1* expression was measured by qPCR. *n* = 3 independent experiments. *E*, isogenic HCT116, RKO, and SW48 colorectal cancer cells (genotype *TP53*<sup>+/+</sup> or *TP53*<sup>-/-</sup>) were treated with 10  $\mu$ M nutlin-3 for 24 h. *GLI1* transcripts were quantified by qPCR, and the results are expressed as the -fold change in treated versus untreated cells. *n* = 3 replicates. *F*, hTERT-RPE1 cells stably expressing an inducible *PTCH53* targeting shRNA were treated with doxycycline for 96 h. DMSO or nutlin-3 (10  $\mu$ M) was added for the final 24 h of shRNA induction, as indicated. *PTCH53* and *GLI1* transcript levels were determined by qPCR. *n* > 3 replicates/sample. *G*, CCD18-Co cells were treated as in *F*. *n* > 3 replicates/sample. Error bars, S.E.

## p53 Activates a PTCH1 Homolog

highly inducible suppressor of Hh signaling. Our analysis showed that the induction of *PTCH53* alone could suppress the activation of GLI-mediated transcription by SMO (Fig. 6, A–C). However, in the cultured cells used in this study, *PTCH53* did not appear to be necessary for the suppression of this pathway by activated p53 (Fig. 7, F and G). One explanation is that there are multiple parallel pathways by which p53 can suppress GLI-mediated transcription. p53 has been implicated in the regulation of GLI1 localization and phosphorylation (28), but the mechanisms that underlie these effects remain poorly defined. Recently, a direct suppressive effect of p53 on Hh signaling has been attributed to the up-regulation of the acetyltransferase p300/CBP-associated factor, an E3 ubiquitin ligase that specifically promotes the degradation of GLI1 protein (29). In contrast, the p53-regulated phosphatase WIP1 has been reported to increase the ability of GLI1 to activate transcription (30). These recent studies suggest that the effects of p53 on canonical Hh signaling are complex and may involve multiple mediators. A requirement for *PTCH53* in the control of canonical Hh signaling might be highly dependent on the specific context in which p53 is activated.

Like *PTCH2* and *PTCHD1* (31, 32), *PTCH53* appears to be a less efficient suppressor of SMO-mediated GLI1 activation than *PTCH1* (Fig. 4C). It is possible that *PTCH53*, *PTCH2*, and *PTCHD1* play auxiliary roles in Hh pathway repression that are specific to distinct physiologic states. In addition to its role in the canonical regulation of GLI-mediated transcription, *PTCH1* has been shown to be involved in GLI-independent pathways (21). Similarly, p53 and *PTCH53* might be involved in a non-canonical pathway that remains to be characterized.

An emerging question is whether inactivating *TP53* mutations could account for the active Hh signaling observed in the many cancers that harbor no other mutations in the Hh pathway. Loss of functional p53 and evidence of Hh pathway activation often coincide in many cancers. It is interesting that in medulloblastoma, a type of brain tumor that typically harbors a very small number (zero to two) of driver mutations (33), *TP53* mutations are most often found in the molecular subtype defined by active Hh signaling and appear to occur exclusively in tumors that lack *PTCH1* mutations (34). New genetic models will be needed to definitively determine whether *TP53* has a role in maintaining the Hh pathway in its normal inactive state in differentiated tissues of the adult.

*Acknowledgments*—We thank Bert Vogelstein, Prasad Jallepalli, James Kim, Stephen Elledge, Craig Peacock, Pao Tien Chuang, John Vincent, Takashi Shimokawa, and Chen Ming Fan for providing critical reagents.

## REFERENCES

1. Wei, C. L., Wu, Q., Vega, V. B., Chiu, K. P., Ng, P., Zhang, T., Shahab, A., Yong, H. C., Fu, Y., Weng, Z., Liu, J., Zhao, X. D., Chew, J. L., Lee, Y. L., Kuznetsov, V. A., Sung, W. K., Miller, L. D., Lim, B., Liu, E. T., Yu, Q., Ng, H. H., and Ruan, Y. (2006) A global map of p53 transcription-factor binding sites in the human genome. *Cell* **124**, 207–219
2. Botcheva, K., McCorkle, S. R., McCombie, W. R., Dunn, J. J., and Anderson, C. W. (2011) Distinct p53 genomic binding patterns in normal and cancer-derived human cells. *Cell Cycle* **10**, 4237–4249
3. Nikulenkov, F., Spinnler, C., Li, H., Tonelli, C., Shi, Y., Turunen, M., Kiv-  
joja, T., Ignatiev, I., Kel, A., Taipale, J., and Selivanova, G. (2012) Insights into p53 transcriptional function via genome-wide chromatin occupancy and gene expression analysis. *Cell Death Differ.* **19**, 1992–2002
4. Riley, T., Sontag, E., Chen, P., and Levine, A. (2008) Transcriptional control of human p53-regulated genes. *Nat. Rev. Mol. Cell Biol.* **9**, 402–412
5. el-Deiry, W. S., Tokino, T., Velculescu, V. E., Levy, D. B., Parsons, R., Trent, J. M., Lin, D., Mercer, W. E., Kinzler, K. W., and Vogelstein, B. (1993) WAF1, a potential mediator of p53 tumor suppression. *Cell* **75**, 817–825
6. Miyashita, T., and Reed, J. C. (1995) Tumor suppressor p53 is a direct transcriptional activator of the human bax gene. *Cell* **80**, 293–299
7. Bieging, K. T., and Attardi, L. D. (2012) Deconstructing p53 transcriptional networks in tumor suppression. *Trends Cell Biol.* **22**, 97–106
8. Parikh, N., Hilsenbeck, S., Creighton, C. J., Dayaram, T., Shuck, R., Shinbrot, E., Xi, L., Gibbs, R. A., Wheeler, D. A., and Donehower, L. A. (2014) Effects of TP53 mutational status on gene expression patterns across 10 human cancer types. *J. Pathol.* **232**, 522–533
9. Miller, L. D., Smeds, J., George, J., Vega, V. B., Vergara, L., Ploner, A., Pawitan, Y., Hall, P., Klaar, S., Liu, E. T., and Bergh, J. (2005) An expression signature for p53 status in human breast cancer predicts mutation status, transcriptional effects, and patient survival. *Proc. Natl. Acad. Sci. U.S.A.* **102**, 13550–13555
10. Sur, S., Pagliarini, R., Bunz, F., Rago, C., Diaz, L. A., Jr., Kinzler, K. W., Vogelstein, B., and Papadopoulos, N. (2009) A panel of isogenic human cancer cells suggests a therapeutic approach for cancers with inactivated p53. *Proc. Natl. Acad. Sci. U.S.A.* **106**, 3964–3969
11. Garnett, M. J., Edelman, E. J., Heidorn, S. J., Greenman, C. D., Dastur, A., Lau, K. W., Greninger, P., Thompson, I. R., Luo, X., Soares, J., Liu, Q., Iorio, F., Surdez, D., Chen, L., Milano, R. J., Bignell, G. R., Tam, A. T., Davies, H., Stevenson, J. A., Barthorpe, S., Lutz, S. R., Kogera, F., Lawrence, K., McLaren-Douglas, A., Mitropoulos, X., Mironenko, T., Thi, H., Richardson, L., Zhou, W., Jewitt, F., Zhang, T., O'Brien, P., Boisvert, J. L., Price, S., Hur, W., Yang, W., Deng, X., Butler, A., Choi, H. G., Chang, J. W., Baselga, J., Stamenkovic, I., Engelman, J. A., Sharma, S. V., Delattre, O., Saez-Rodriguez, J., Gray, N. S., Settleman, J., Futreal, P. A., Haber, D. A., Stratton, M. R., Ramaswamy, S., McDermott, U., and Benes, C. H. (2012) Systematic identification of genomic markers of drug sensitivity in cancer cells. *Nature* **483**, 570–575
12. Barretina, J., Caponigro, G., Stransky, N., Venkatesan, K., Margolin, A. A., Kim, S., Wilson, C. J., Lehár, J., Kryukov, G. V., Sonkin, D., Reddy, A., Liu, M., Murray, L., Berger, M. F., Monahan, J. E., Morais, P., Meltzer, J., Korjawa, A., Jané-Valbuena, J., Mapa, F. A., Thibault, J., Bric-Furlong, E., Raman, P., Shipway, A., Engels, I. H., Cheng, J., Yu, G. K., Yu, J., Aspesi, P., Jr., de Silva, M., Jagtap, K., Jones, M. D., Wang, L., Hatton, C., Palesscandolo, E., Gupta, S., Mahan, S., Sougnez, C., Onofrio, R. C., Liefeld, T., MacConaill, L., Winckler, W., Reich, M., Li, N., Mesirov, J. P., Gabriel, S. B., Getz, G., Ardlie, K., Chan, V., Myer, V. E., Weber, B. L., Porter, J., Warmuth, M., Finan, P., Harris, J. L., Meyerson, M., Golub, T. R., Morrissey, M. P., Sellers, W. R., Schlegel, R., and Garraway, L. A. (2012) The Cancer Cell Line Encyclopedia enables predictive modelling of anticancer drug sensitivity. *Nature* **483**, 603–607
13. Gao, J., Aksoy, B. A., Dogrusoz, U., Dresdner, G., Gross, B., Sumer, S. O., Sun, Y., Jacobsen, A., Sinha, R., Larsson, E., Cerami, E., Sander, C., and Schultz, N. (2013) Integrative analysis of complex cancer genomics and clinical profiles using the cBioPortal. *Sci. Signal.* **6**, pii
14. Meerbrey, K. L., Hu, G., Kessler, J. D., Roarty, K., Li, M. Z., Fang, J. E., Herschkowitz, J. I., Burrows, A. E., Ciccio, A., Sun, T., Schmitt, E. M., Bernardi, R. J., Fu, X., Bland, C. S., Cooper, T. A., Schiff, R., Rosen, J. M., Westbrook, T. F., and Elledge, S. J. (2011) The pINDUCER lentiviral toolkit for inducible RNA interference *in vitro* and *in vivo*. *Proc. Natl. Acad. Sci. U.S.A.* **108**, 3665–3670
15. Hausmann, G., von Mering, C., and Basler, K. (2009) The hedgehog signaling pathway: where did it come from? *PLoS Biol.* **7**, e1000146
16. el-Deiry, W. S., Kern, S. E., Pietenpol, J. A., Kinzler, K. W., and Vogelstein, B. (1992) Definition of a consensus binding site for p53. *Nat. Genet.* **1**, 45–49
17. Hoh, J., Jin, S., Parrado, T., Edington, J., Levine, A. J., and Ott, J. (2002) The p53MH algorithm and its application in detecting p53-responsive genes.

- Proc. Natl. Acad. Sci. U.S.A.* **99**, 8467–8472
18. Kent, W. J. (2002) BLAT—the BLAST-like alignment tool. *Genome Res.* **12**, 656–664
  19. ENCODE Project Consortium, Bernstein, B. E., Birney, E., Dunham, I., Green, E. D., Gunter, C., and Snyder, M. (2012) An integrated encyclopedia of DNA elements in the human genome. *Nature* **489**, 57–74
  20. Kandoth, C., McLellan, M. D., Vandin, F., Ye, K., Niu, B., Lu, C., Xie, M., Zhang, Q., McMichael, J. F., Wyczalkowski, M. A., Leiserson, M. D., Miller, C. A., Welch, J. S., Walter, M. J., Wendl, M. C., Ley, T. J., Wilson, R. K., Raphael, B. J., and Ding, L. (2013) Mutational landscape and significance across 12 major cancer types. *Nature* **502**, 333–339
  21. Robbins, D. J., Fei, D. L., and Riobo, N. A. (2012) The Hedgehog signal transduction network. *Sci. Signal.* **5**, re6
  22. Barakat, M. T., Humke, E. W., and Scott, M. P. (2010) Learning from Jekyll to control Hyde: Hedgehog signaling in development and cancer. *Trends Mol. Med.* **16**, 337–348
  23. Chung, J. H., and Bunz, F. (2013) A loss-of-function mutation in PTCH1 suggests a role for autocrine hedgehog signaling in colorectal tumorigenesis. *Oncotarget* **4**, 2208–2211
  24. Triscott, J., Lee, C., Foster, C., Manoranjan, B., Pambid, M. R., Berns, R., Fotovati, A., Venugopal, C., O'Halloran, K., Narendran, A., Hawkins, C., Ramaswamy, V., Bouffet, E., Taylor, M. D., Singhal, A., Hukin, J., Rassekh, R., Yip, S., Northcott, P., Singh, S. K., Dunham, C., and Dunn, S. E. (2013) Personalizing the treatment of pediatric medulloblastoma: Polo-like kinase 1 as a molecular target in high-risk children. *Cancer Res.* **73**, 6734–6744
  25. Sasai, K., Romer, J. T., Lee, Y., Finkelstein, D., Fuller, C., McKinnon, P. J., and Curran, T. (2006) Shh pathway activity is down-regulated in cultured medulloblastoma cells: implications for preclinical studies. *Cancer Res.* **66**, 4215–4222
  26. Colvin Wanshura, L. E., Galvin, K. E., Ye, H., Fernandez-Zapico, M. E., and Wetmore, C. (2011) Sequential activation of Snail1 and N-Myc modulates sonic hedgehog-induced transformation of neural cells. *Cancer Res.* **71**, 5336–5345
  27. Taipale, J., Chen, J. K., Cooper, M. K., Wang, B., Mann, R. K., Milenkovic, L., Scott, M. P., and Beachy, P. A. (2000) Effects of oncogenic mutations in Smoothened and Patched can be reversed by cyclopamine. *Nature* **406**, 1005–1009
  28. Stecca, B., and Ruiz i Altaba, A. (2009) A GLI1-p53 inhibitory loop controls neural stem cell and tumour cell numbers. *EMBO J.* **28**, 663–676
  29. Mazzà, D., Infante, P., Colicchia, V., Greco, A., Alfonsi, R., Siler, M., Antonucci, L., Po, A., De Smaele, E., Ferretti, E., Capalbo, C., Bellavia, D., Canettieri, G., Giannini, G., Screpanti, I., Gulino, A., and Di Marcotullio, L. (2013) PCAF ubiquitin ligase activity inhibits Hedgehog/Gli1 signaling in p53-dependent response to genotoxic stress. *Cell Death Differ.* **20**, 1688–1697
  30. Pandolfi, S., Montagnani, V., Penachioni, J.Y., Vinci, M.C., Olivito, B., Borgognoni, L., and Stecca, B. (2013) WIP1 phosphatase modulates the Hedgehog signaling by enhancing GLI1 function. *Oncogene* **32**, 4737–4747
  31. Lee, Y., Miller, H. L., Russell, H. R., Boyd, K., Curran, T., and McKinnon, P. J. (2006) Patched2 modulates tumorigenesis in patched1 heterozygous mice. *Cancer Res.* **66**, 6964–6971
  32. Noor, A., Whibley, A., Marshall, C. R., Gianakopoulos, P. J., Piton, A., Carson, A. R., Orlic-Milacic, M., Lionel, A. C., Sato, D., Pinto, D., Drmic, I., Noakes, C., Senman, L., Zhang, X., Mo, R., Gauthier, J., Crosbie, J., Pagnamenta, A. T., Munson, J., Estes, A. M., Fiebig, A., Franke, A., Schreiber, S., Stewart, A. F., Roberts, R., McPherson, R., Guter, S. J., Cook, E. H., Jr., Dawson, G., Schellenberg, G. D., Battaglia, A., Maestrini, E., Autism Genome Project, C., Jeng, L., Hutchison, T., Rajcan-Separovic, E., Chudley, A. E., Lewis, S. M., Liu, X., Holden, J. J., Fernandez, B., Zwaigenbaum, L., Bryson, S. E., Roberts, W., Szatmari, P., Gallagher, L., Stratton, M. R., Geicz, J., Brady, A. F., Schwartz, C. E., Schachar, R. J., Monaco, A. P., Rouleau, G. A., Hui, C. C., Lucy Raymond, F., Scherer, S. W., and Vincent, J. B. (2010) Disruption at the PTCHD1 locus on Xp22.11 in autism spectrum disorder and intellectual disability. *Sci. Trans. Med.* **2**, 49ra68
  33. Vogelstein, B., Papadopoulos, N., Velculescu, V. E., Zhou, S., Diaz, L. A., Jr., and Kinzler, K. W. (2013) Cancer genome landscapes. *Science* **339**, 1546–1558
  34. Jones, D. T., Jäger, N., Kool, M., Zichner, T., Hutter, B., Sultan, M., Cho, Y. J., Pugh, T. J., Hovestadt, V., Stütz, A. M., Rausch, T., Warnatz, H. J., Ryzhova, M., Bender, S., Sturm, D., Pleier, S., Cin, H., Pfaff, E., Sieber, L., Wittmann, A., Remke, M., Witt, H., Hutter, S., Tzaridis, T., Weischenfeldt, J., Raeder, B., Avci, M., Amstislavskiy, V., Zapatka, M., Weber, U. D., Wang, Q., Lasitschka, B., Bartholomae, C. C., Schmidt, M., von Kalle, C., Ast, V., Lawerenz, C., Eils, J., Kabbe, R., Benes, V., van Sluis, P., Koster, J., Volckmann, R., Shih, D., Betts, M. J., Russell, R. B., Coco, S., Tonini, G. P., Schüller, U., Hans, V., Graf, N., Kim, Y. J., Monoranu, C., Roggendorf, W., Unterberg, A., Herold-Mende, C., Milde, T., Kulozik, A. E., von Deimling, A., Witt, O., Maass, E., Rossler, J., Ebinger, M., Schuhmann, M. U., Fruhwald, M. C., Hasselblatt, M., Jabado, N., Rutkowski, S., von Bueren, A. O., Williamson, D., Clifford, S. C., McCabe, M. G., Collins, V. P., Wolf, S., Wiemann, S., Lehrach, H., Brors, B., Scheurlen, W., Felsberg, J., Reifenberger, G., Northcott, P. A., Taylor, M. D., Meyerson, M., Pomeroy, S. L., Yaspo, M. L., Korbel, J. O., Korshunov, A., Eils, R., Pfister, S. M., and Lichter, P. (2012) Dissecting the genomic complexity underlying medulloblastoma. *Nature* **488**, 100–105
  35. Krogh, A., Larsson, B., von Heijne, G., and Sonnhammer, E. L. (2001) Predicting transmembrane protein topology with a hidden Markov model: application to complete genomes. *J. Mol. Biol.* **305**, 567–580